Applied Water Science (2022) 12: 215
https://doi.org/10.1007/s13201-022-01737-w

ORIGINAL ARTICLE

Numerical simulation of flow on circular crested stepped spillway

Abbas Parsaie[1] · Saleh Jaafer Suleiman Shareef[2] · Amir Hamzeh Haghiabi[3] · Raad Hoobi Irzooki[4] · Rasul M. Khalaf[5]

Received: 11 May 2022 / Accepted: 6 July 2022 / Published online: 2 August 2022

Abstract

The spillways are one of the most important hydraulic structures used in river engineering, dam construction, irrigation, and drainage engineering projects. Recently, a new type of such spillways with a circular crest has been proposed. In this paper, the hydraulic properties of the circular crested stepped spillway (CCSS) including flow pattern, distribution of velocity on the crest and pressure, turbulence intensity, discharge coefficient (C_d) and energy dissipation ratio (EDR) were investigated numerically. To model the free surface of flow the volume of fluid technique, and for modeling the turbulence of flow, $\mathrm{k}-\varepsilon$ (RNG) was utilized. Results declared that there is a good agreement between the laboratory observations and numerical simulation. The C_d of the CCSS changes between 0.9 and 1.4 considering the range of relative upstream head (h_{up}/R) between 0.33 m and 2.67. The observation of the flow streamlines showed that they are tangential to the curvature of the crest and there is no separation of the flow from the crest. Examination of the pressure distribution on the CCSS model shows that just downstream part of the crest, the pressure is partially negative. Of course, the same partial negative pressure is observed on the edge of the steps. The steps increase the maximum intensity turbulence by 50%. The CCSS can dissipate the energy of flow between 90 and 30%, and in the skimming flow regime, the portion of each step in the energy dissipation regardless of their position is almost identical.

Keywords CFD simulation · Discharge capacity · Energy dissipation · Skimming flow · Spillway

List of symbols

h_s	Height of steps
h_{up}	Head of flow over
C_d	Discharge coefficient
H_{dwn}	Total head of flow at upstream of spillway
H_{up}	Total head of flow downstream of the spillway
L_s	Length of steps
V_1	Flow velocity downstream of the spillway
V_{up}	Flow velocity at upstream of spillway
y_{up}	Depth of flow over
CCSS	Circular crested stepped spillway
CFD	Computational fluid dynamic
EDR	Energy dissipation ratio
N	Number of steps
S	Slope of chute
V	H: Vertical: horizontal
VOF	Volume of fluid
yc	Critical depth of flow
P	Height of spillway
R	Radius of crest
g	Acceleration due to gravity
q	Discharge per width

✉ Abbas Parsaie
parsaie@scu.ac.ir

Saleh Jaafer Suleiman Shareef
salehjaafer@ntu.edu.iq

Amir Hamzeh Haghiabi
ahaghiabi@gmail.com

Raad Hoobi Irzooki
dr.raadhoobi@tu.edu.iq

Rasul M. Khalaf
rasulcon@uomustansiriyah.edu.iq

1 Shahid Chamran University of Ahvaz, Ahvaz, Iran

2 Water Resources Engineering, Northern Technical University, Engineering Technical College, Mosul, Iraq

3 Water Engineering Department, Lorestan University, Khorramabad, Iran

4 Water Resources Engineering, Environmental Engineering Department, Tikrit University, Tikrit, Iraq

5 Water Resources Engineering, Civil Engineering Department, Al-Mustansiriyah University, Baghdad, Iraq

Introduction

Modeling the important hydraulic structures such as spillways always is one of the fundamental steps in hydraulic engineering projects such as dam construction and river diversion works. The design of spillways in each project according to their specific conditions can be a unique case. Although there are technical manuals for designing spillways, the final plan should be tested using a physical model (Hager and Pfister 2010; Bagheri and Kabiri-Samani 2020a; Haghiabi et al. 2018). The modeling aims to investigate the hydraulic properties including the flow pattern, discharge capacity (determine the rating curve), and distribution of velocity and pressure of flow through the spillway. Over the past decades, the hydraulic properties of various components of the spillway, including the guide walls (Wang and Chen 2010), approach channel (Zhang et al. 2015; Parsaie et al. 2018), crest (Mohammadzadeh-Habili et al. 2016; Shamsi et al. 2022; Parsaie and Haghiabi 2021), chute (Parsaie et al. 2016) and energy dissipator located at the toe of the chute (Valero et al. 2018), have been investigated using physical and numerical simulation. Today, the use of numerical simulation as a powerful tool in the design of spillways and evaluation of their alternative plans is common. In this regard, numerous studies have been published, most of which confirm the accuracy of numerical modeling results (Ghaderi et al. 2020a, 2020b; Rahimzadeh et al. 2012; Tadayon and Ramamurthy 2009; Bai et al. 2017; Zhan et al. 2016; Mohammad Rezapour Tabari and Tavakoli 2016; Bagheri and Kabiri-Samani 2020b). The velocity of the flow on the spillway's chute is very high, which increases the risk of cavitation as well as scouring downstream of the spillway. Spreading downstream scour to the toe of the spillway may damage the dam body (Nou et al. 2021; Ghaderi et al. 2020b; Haghiabi 2017; Samadi et al. 2015). One of the effective ways to dissipate the energy of the flow passing through the spillway's chute is to step its surface (Parsaie and Haghiabi 2019a), which both cause energy dissipation and increase the aeration of the flow (Parsaie and Haghiabi 2019c).

Recently, a circular crest stepped spillway (CCSS) due to having high C_d, suitable ability in energy dissipation and flow aeration has been proposed (Parsaie and Haghiabi 2019b). Hence, in this study, the hydraulic properties of the CCSS including flow pattern according to the flow streamlines, the distribution of flow velocity on the crest and pressure on the stepped chute, and energy dissipation are investigated using computational fluid dynamic (CFD) method.

Materials and methods

A CCSS consists of a circular crest that its curvature is an arc of a circle as well as a downstream stepped chute. The CCSS as shown in Fig. 1 is categorized as a short crested weir. In this figure, h_s and L_s are the height and length of step, respectively. R is the radius of crest. P is the height of spillway. h_{up} and y_{up} are the head and depth of flow over the crest upstream. Equation 1 can demonstrate the discharge capacity of the short crested weirs (Bos 1976). In this equation, q is the discharge per width, g is acceleration due to gravity, and C_d is the discharge coefficient.

$$q = \frac{2}{3} C_d h_{up} \sqrt{\frac{2}{3} g h_{up}} \tag{1}$$

To estimate the performance of CCSS regarding energy dissipation, the total head of flow downstream (Eq. 2:H_{dwn}) mins the total head flow upstream (Eq. 2:H_{up}). The ratio of their difference to the H_{up} (Eq. 4) is defined as the performance of CCSS regarding energy dissipation (Haghiabi et al. 2022).

Fig. 1 The sketch of the stepped spillway with circular crest

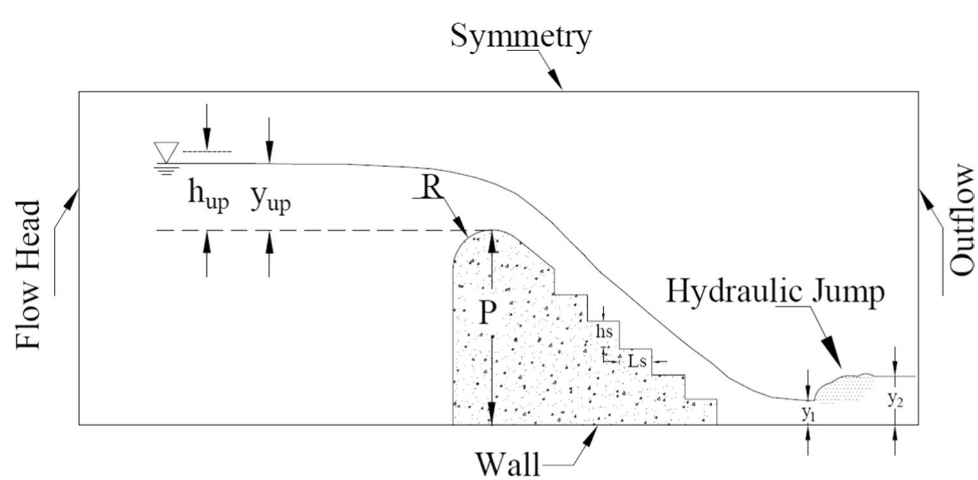

$$H_{up} = P + y_{up} + \frac{V_{up}^2}{2g} = P + y_{up} + \frac{q^2}{2g(P + y_{up})^2} \quad (2)$$

$$H_{dwn} = y_1 + \frac{V_1^2}{2g} = y_1 + \frac{q^2}{2gy_1^2} \quad (3)$$

$$\frac{\Delta H}{H_{up}} = \frac{H_{up} - H_{dwn}}{H_{up}} = \left(1 - \frac{H_{dwn}}{H_{up}}\right) \times 100 \quad (4)$$

where the V_{up} and V_1 are the flow velocity at the upstream and downstream of the CCSS.

Experimental setups

The laboratory investigation on hydraulic models of the CCSS was carried out in a flume of 12 m long, 0.5 m wide and 0.45 m deep. The sidewalls of the flume were made of Plexiglas. The water surface profile in the flume was measured using a point gauge. The flow discharge was measured by a calibrated triangular weir located at the end of the flume. The height of the models was 0.3 m. The radius of the crest of the models was considered to be 0.06 m. The slope of the downstream step chute equal to (V: H) was 1:1.25. The models were made of concrete. The details of the smooth and CCSS models and the range of discharge of flow during the test are presented in Table 1.

CFD modeling

In this study, the numerical modeling of hydraulic properties of flow over the CCSS was performed using Flow 3D. The Flow 3D uses the finite volume method for the discretization of the governing equations of flow (Navier–Stokes equations). The strategy of this software to discretize the computational domain is using the structured mesh. The volume of fluid (VOF) method is utilized for modeling the free surface of the flow. The standard flow equations such as continuity equations (Eq. 5) and Navier–Stokes equations (Eq. 6) are solved numerically for all computational domains (Moukalled et al. 2015; Parsaie et al. 2016).

$$v_f \frac{\partial \rho}{\partial t} + \frac{\partial}{\partial x}(uA_x) + \frac{\partial}{\partial x}(vA_y) = \frac{PSOR}{\rho} \quad (5)$$

where u, v, z are the velocity components in the x, y and w directions. A_x, A_y are the cross-sectional area of the flow, ρ is fluid density, $PSOR$ is the source term, v_f is the volume fraction of the fluid and three-dimensional momentum equations given in Eq. (6).

$$\frac{\partial u}{\partial t} + \frac{1}{v_f}\left(uA_x\frac{\partial u}{\partial x} + vA_y\frac{\partial u}{\partial y} + wA_z\frac{\partial u}{\partial z}\right) = -\frac{1}{\rho}\frac{\partial P}{\partial x} + G_x + f_x$$
$$\frac{\partial v}{\partial t} + \frac{1}{v_f}\left(uA_x\frac{\partial v}{\partial x} + vA_y\frac{\partial v}{\partial y} + wA_z\frac{\partial v}{\partial z}\right) = -\frac{1}{\rho}\frac{\partial P}{\partial y} + G_y + f_y \quad (6)$$

where P is the fluid pressure, G_x, G_y the acceleration created by body fluids, f_x, f_y viscosity acceleration in three dimensions and v_f is related to the volume of fluid, defined by Eq. (7). For modeling of free surface profile, the VOF technique based on the volume fraction of the computational cells has been used. Since the volume fraction F represents the amount of fluid in each cell, it takes a value between 0 and 1.

$$\frac{\partial F}{\partial t} + \frac{1}{v_f}\left[\frac{\partial}{\partial x}(FA_x u) + \frac{\partial}{\partial y}(FA_y v)\right] = 0 \quad (7)$$

To model turbulent flow, numbers of turbulence models including one-equation turbulent model (Prandtl mixing length), two types of two-equation k-ε models, renormalized group model (RNG- k-ε) and large-eddy simulation (LES) have been proposed. The RNG- k-ε model is a powerful turbulence model that has suitable performance for modeling the fine vortex; therefore, this model is very useful for modeling flow pattern problems. Most equations used in the RNG model are given in Eqs. (8 and 9).

$$\frac{\partial}{\partial t}(\rho k) + \frac{\partial}{\partial x}(\rho u_i k) = \frac{\partial}{\partial x_i}\left(\alpha_k \mu_{eff}\frac{\partial k}{\partial x_i}\right) + G_k + G_b - \rho\varepsilon \quad (8)$$

$$\frac{\partial}{\partial t}(\rho\varepsilon) + \frac{\partial}{\partial x}(\rho u_i \varepsilon) = \frac{\partial}{\partial x_i}\left(\alpha_k \mu_{eff}\frac{\partial \varepsilon}{\partial x_i}\right) + C_{1\varepsilon}\frac{\varepsilon}{k}(G_k + C_{3\varepsilon}G_b) - C_{2\varepsilon}\rho\frac{\varepsilon^2}{k} - R \quad (9)$$

in which G_k is the rate of kinetic energy creation, and R is the density of turbulence defined as below.

Table 1 The details of the CCSS models and flow rate

Model	R (m)	P (m)	N	S (V:H)	Q (m³/s)
Smooth spillway	0.06	0.3	–	1:1.25	0.003–0.045
				1:1.25	
Stepped spillway	0.06	0.3	3,5 and 7	1:1	
				1:0.75	

$$R = \frac{C_\mu \rho \eta^3 (1 - \eta/\eta_0)}{1 + \beta \eta^3} \frac{\varepsilon^2}{k}, \quad \mu_t = \rho C_\mu \frac{k^2}{\varepsilon} \tag{10}$$

In these equations $\beta = 0.012, \eta_0 = 1.38$.

CFD model Setup

To simulate the flow over the CCSS, the number of steps including the definition of the two-dimensional models, definition and meshing of the computational domain, setting the boundary and initial conditions, and selecting the turbulence model should be followed. In this case, the upstream flow head and output were selected as the upstream and downstream boundary conditions, respectively. The symmetry was chosen as the boundary condition of the upper faces of the computational domain. For the lower face of the computational domain, the wall boundary condition was chosen. In this study, the $k-\varepsilon$ (RNG) model is used as the turbulence model. The size of the meshes was equal to 1.0 cm (horizontal) × 0.5 cm(vertical). These mesh dimensions are chosen to meet the criteria of mesh independence.

Results and discussion

In this section, the results of numerical simulation are presented. For Flow 3D validation, the water surface profile, flow head and flow discharge were used. Figure 2 shows the measured water surface profile and the results of numerical simulation in the validation stage.

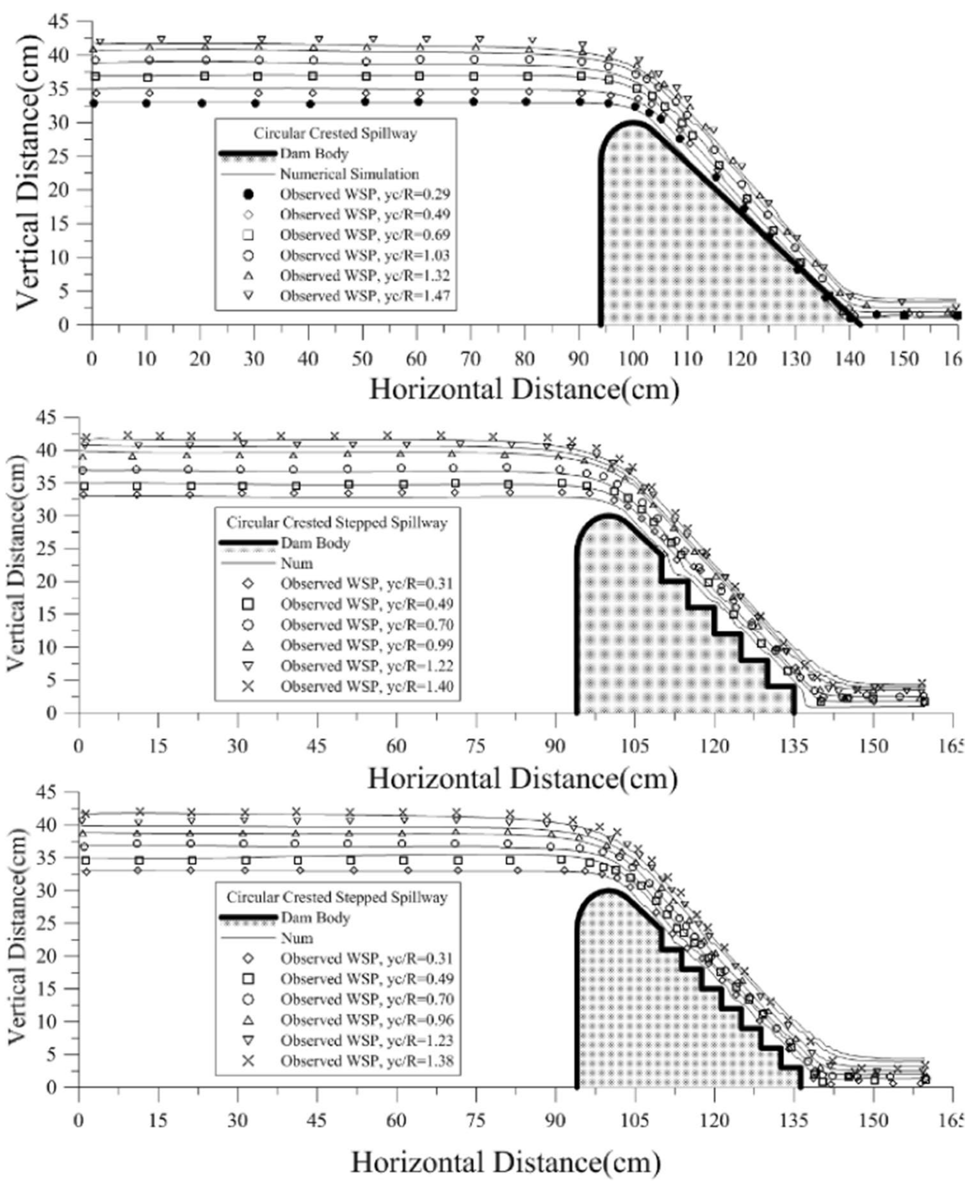

Fig. 2 The results of the measured water surface profile and the numerical simulation

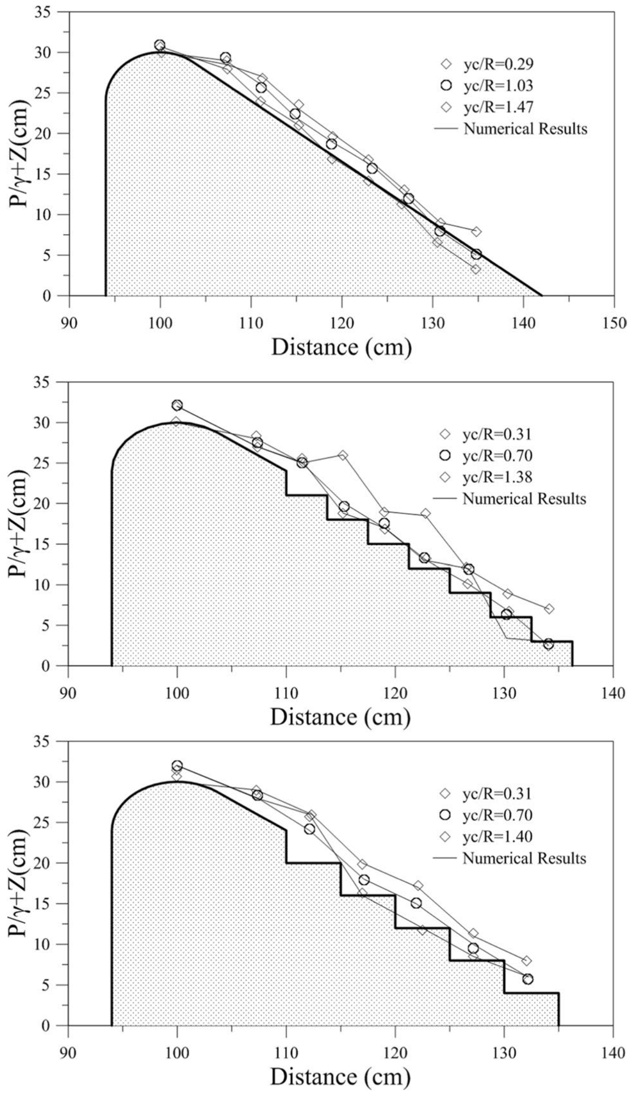

Fig. 3 The results of the measured piezometric pressure and the numerical simulation

In this stage, the measured piezometric pressure and results of numerical simulation are plotted in Fig. 3. In these figures, the calibration results for the smooth and stepped model are shown. The examination of the calibration results shows that there is good agreement between the numerical results and the laboratory measurements.

In Fig. 4a and b, the measured discharge capacity, discharge coefficient (C_d) and the results of numerical simulations are shown, as well. In this figure, only the size of the steps is changed and it has been attempted to consider the slope of the stepped chute as constant. This figure shows that the geometric properties of the steps including size and slope of steps do not affect the discharge coefficient and the stage–discharge relation. These results support the theory of supercritical flow which defines that in the supercritical flow, the downstream cannot affect the upstream flow properties.

One of the most important reasons for the high value of C_d of CCSS is the curvature of its crest. This curvature prevents the separation of the streamlines from the surface of the crest and results in a significant reduction in the energy loss of the flow passing over the crest part. Figure 5 shows the streamlines over the CCSS. As shown in this figure, all the streamlines are tangential to the curvature of the crest surface. Figure 5b shows the streamlines on the stepped chute. As can be seen from this figure, a vortex flow is formed between the stairs, which also reduces the flow energy. The examination of Fig. 5a shows that the flow regime at the upstream part of the crest is subcritical and the other part (downstream part) is supercritical. In other words, the critical point is formed on the crest. According to the subcritical flow theory, the crest geometry (crest radius) can affect the C_d. It should be noted that the critical depth increases with increasing flow discharge and scrolls upstream. This means that by increasing the discharge of flow the effect of the

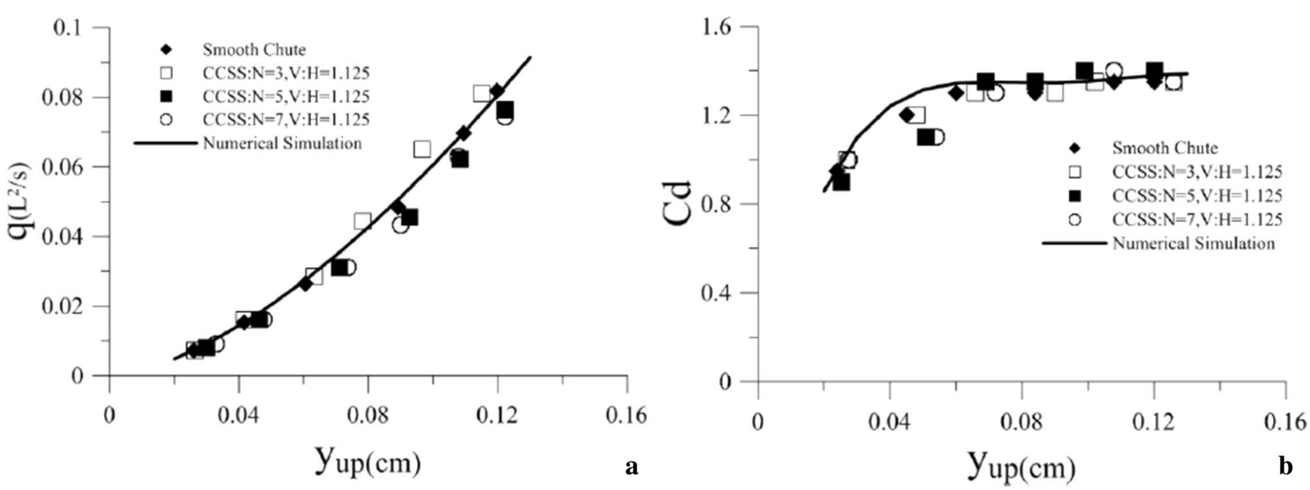

Fig. 4 The results of numerical modeling of stage–discharge (**a**) and discharge coefficient (**b**) of the CCSS

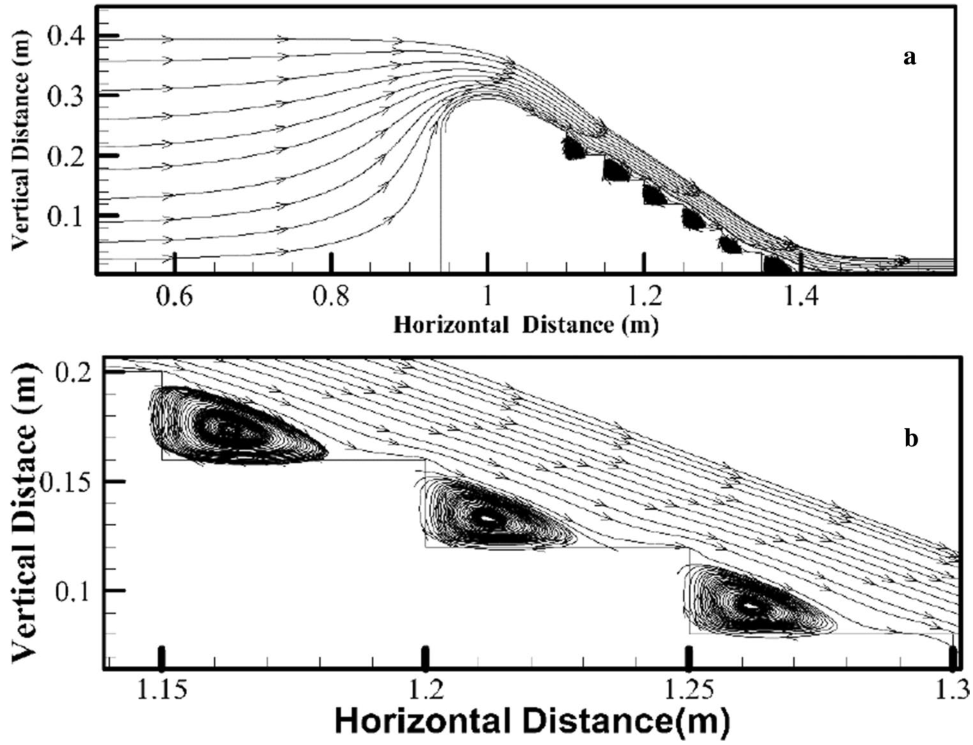

Fig. 5 The streamline and Froude number of flow over the crest (**a**) and chute (**b**) of CCSS

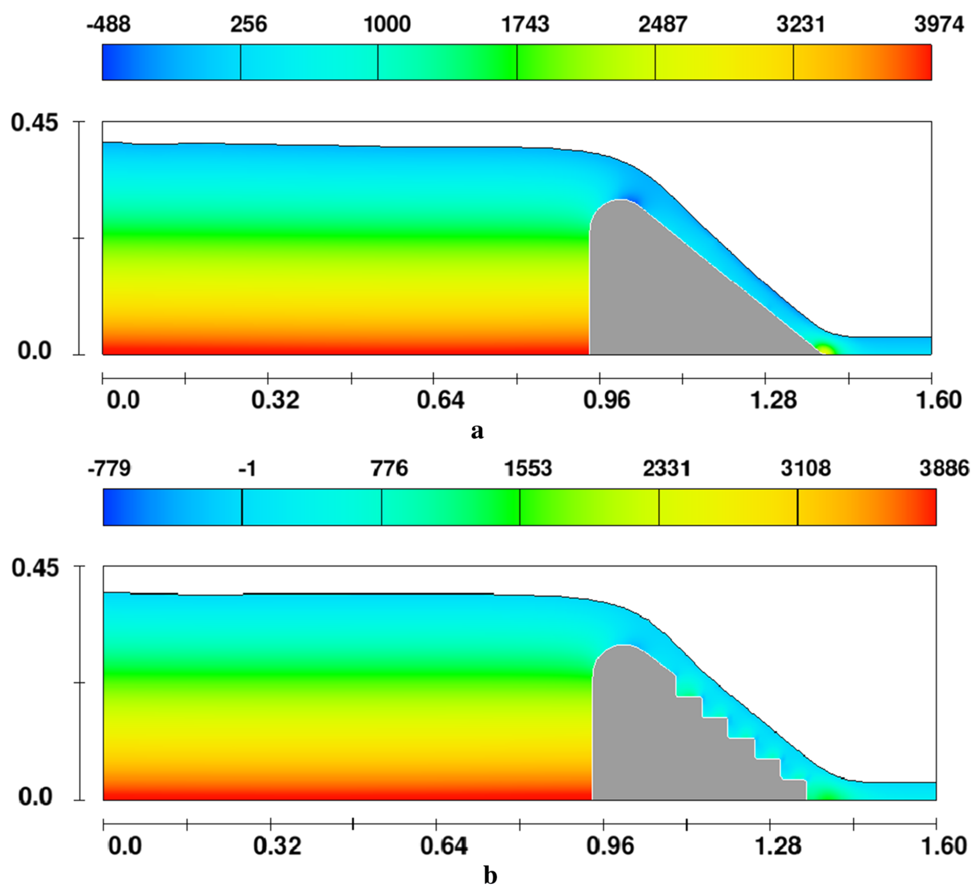

Fig. 6 The distribution of pressure over the smooth (**a**) and stepped chute (**b**)

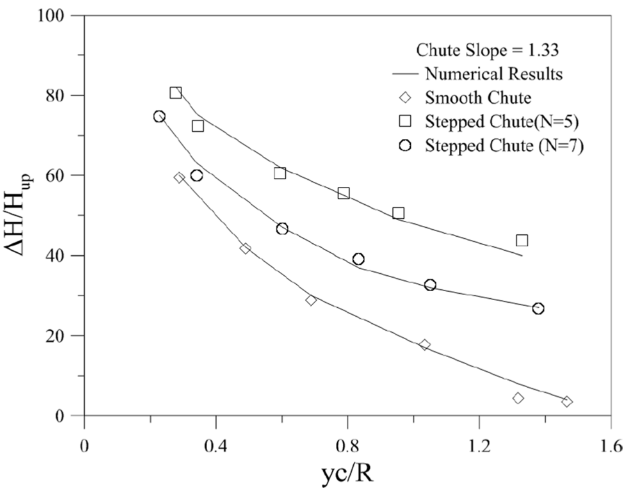

Fig. 7 The energy dissipation of flow on the CCSS

upstream part of the crest on the C_d is decreased. For this reason, as shown in Fig. 4, the C_d remains relatively constant after the y_{up} more than 0.05 m ($y_{up}/R \cong 1$).

Figure 6 illustrates the pressure distribution over the circular crested spillway with a smooth (Fig. 6a) and stepped chute (Fig. 6b). Although the flow velocity at the downstream part of the crest increases, the main cause of the negative pressure zone is the sudden change in the direction of flow velocity and the formation of the wake region. Of course, this decrease in pressure even down to negative pressure values can be justified. It should be noted that the negative pressure in this section does not lead to cavitation and structural degradation. However, it leads to an increase in the discharge capacity due to a rise in the suction zone of flow. This is reminiscent of the criteria of the head design of the Ogee spillway, where the design head can be considered up to 1.5 times the head of the design flood discharge without any problems in the crest part. As the flow passes on the smooth chute, the flow velocity increases, and subsequently, the flow pressure decreases according to the energy equation. As the flow reaches the stilling basin or energy dissipator structure due to the collision of the flow with the surface of the concrete slab, the flow energy dissipation increases. It is noteworthy that the energy dissipation is reflected in the decrease in flow velocity and the amount of pressure at the toe of the chute increases. In the following, the distribution of pressure over the CCSS is investigated. As shown in Fig. 6, the value of pressure on the surface of

Fig. 8 The energy dissipation of flow on the CCSS

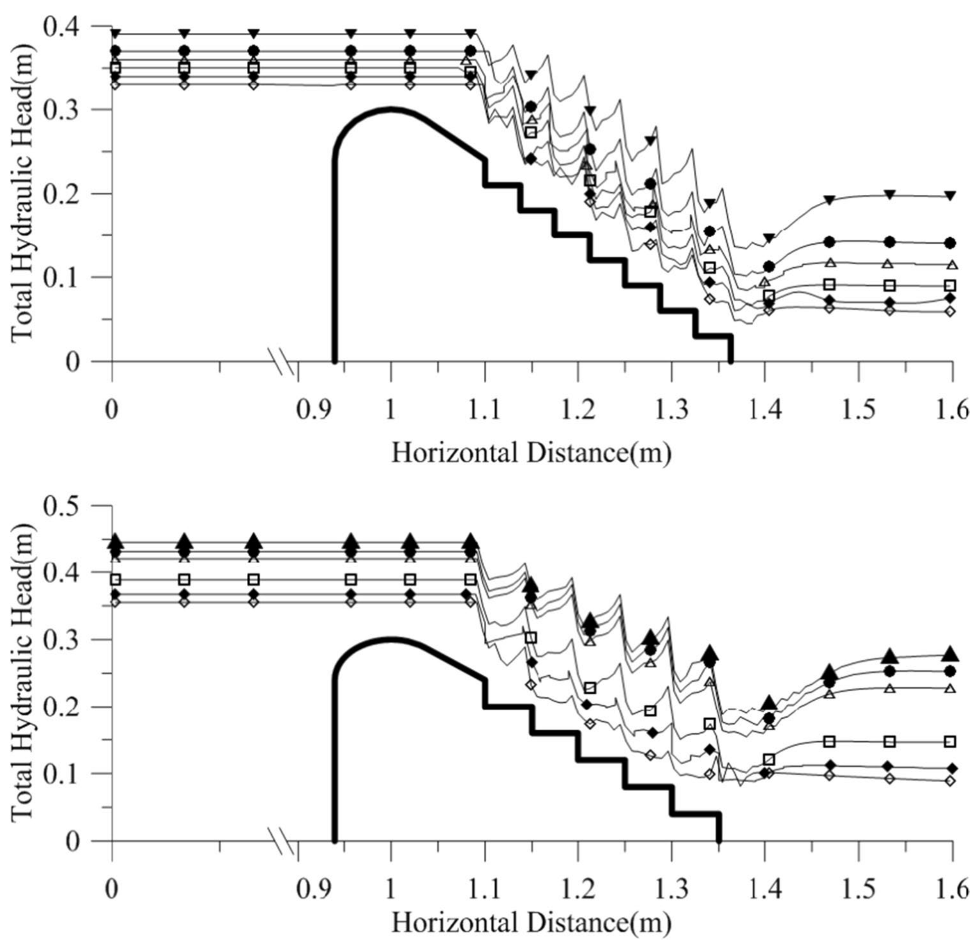

steps is positive and at their edges is negative. Of course, it should be checked whether this amount of negative pressure will damage the structure and how much of it (negative) is allowed. To do this, the cavitation index should be calculated. In other words, this will investigate the potential of the CCSS for cavitation to occur. According to Fig. 6, the inlet flow pressure to the stilling basin downstream of the stepped spillway is lower than that of the smooth chute spillway, which is due to the greater dissipation of the flow energy through the stepped chute. The results show that as the size of the steps increases, the energy dissipation of flow increases. This is because the intensity of the turbulence of the flow increases with the increase of the step size.

The performance of CCSS in terms of energy dissipation is shown in Fig. 7. As presented in this figure, the CCSS can dissipate the flow energy between 90 and 30%. The stepped chute can dissipate energy about 50% more than the smooth chute even in the skimming flow regime. As presented in this figure, by increasing the discharge, the performance of smooth and stepped chute decreases significantly. Of course, the intensity of the reduction of smooth chute performance is more than the stepped chute. In a smooth chute with an increasing flow rate, its performance decreases by about 91%, while in the same range of increasing flow, the performance of a stepped chute decreases by about 37%.

The effect of each part of CCSS including the crest and steps on the energy dissipation is shown in Fig. 8. As shown in this figure the portion of the crest in the energy dissipation is negligible. That reason is the least disturbance in the flow path (streamlines) due to its proper curvature of the crest. When the flow enters the first step, a considerable amount of its energy is dissipated compared to the crest part. At the low value of discharges, the energy loss is due to the collision of the flow with the surface of the steps. By increasing the flow discharge as shown in Fig. 5a, the vortex flow is generated between the steps. The structure of the vertex flows from a larger view is shown in Fig. 5b. After the formation of the vortex flow in the steps, a pseudo-boundary is formed between the steps and the main flow jet that reduces the effect of the steps' size on energy dissipation. This mode of flow is called the skimming flow regime. The h_s/L_s of laboratory models was 0.8, 1.0 and 1.33; hence, when the ratio of y_c/h_s is more than the 0.5, the skimming flow is formed. Theis finding confirms with criteria presented by Rajaratnam (1990), Chamani and Rajaratnam (1999), and James et al. (2001). After the full development of flow on the stepped chute and formation of the skimming flow on the steps, the

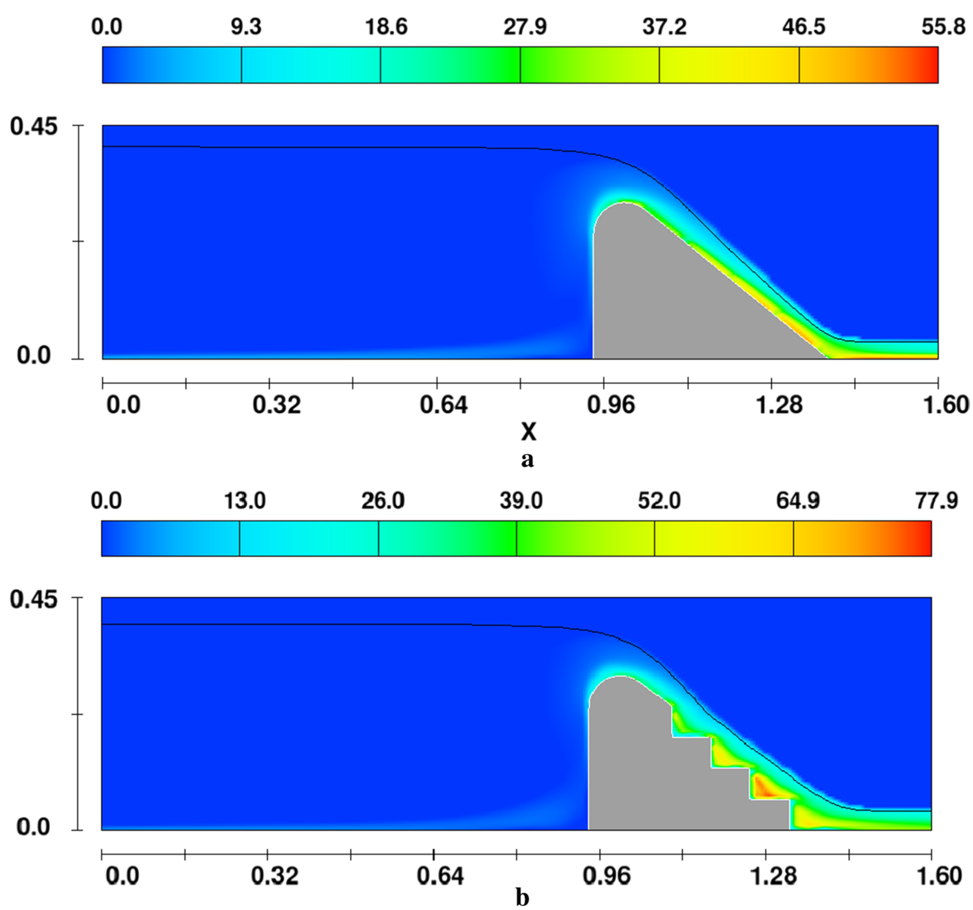

Fig. 9 The distribution of turbulent intensity percentage over the smooth (**a**) and CCSS (**b**)

portion of each of the steps regardless of their position in the energy dissipation is almost identical. In other words, with the increase of the discharge, the contribution of each step to the energy dissipating decreases. Increasing the step size increases the intensity of flow turbulence, which further increases the rate of flow energy dissipation. It should be noted that the total head of flow must decrease during the spillway, but as seen, on each of the steps, the head of flow firstly decreases and then increases. This is because the direction of velocity in the vortex flow that forms on the steps is the opposite of the flow direction. Moving from the vertex flow to the tip of the steps, the direction of flow is synchronized with the overall direction of the flow passing through the stepped chute, As a result, the flow head is increased relative to the areas affected by the vortex flow.

The effect of the step size as the roughness of the chute on the turbulence intensity is shown in Fig. 9c and d. As shown in these figures, the maximum turbulence intensity of flow on the smooth chute is about 40, whereas this value is increased by up to 48 for the smallest steps, and as the steps become larger, this value is increased to about 78. As the size of the steps increases, the intensity of the flow turbulence increases, which in turn increases the amount of energy loss caused by them.

Conclusion

In this study, the hydraulic properties of circular crested stepped spillways including the pattern of streamlines, distribution of pressure, rating curve, discharge coefficient and mechanism of energy dissipation were investigated. Results declared that the length and curvature of the crest make it possible for the streamlines to adapt to the surface of the crest. The results also showed that crest curvature does not lead to dissipation of the flow energy. The downstream part of the crest performs the smooth transfer of flow from the crest to the stepped chute. By the formation of the skimming flow regime, the contribution of the steps to the energy dissipation decreases, and their portion in the energy dissipation is almost identical regardless of their position. As the step size increases, the intensity of the flow turbulence increases, resulting in a greater amount of energy dissipation.

Author contribution Dr. Haghiabi conceived of the presented idea; Dr. Parsaie developed the theory and performed the computations; Dr. Suleiman Shareef, Dr. Irzooki and Dr. Khalaf performed experimental tests.

Funding The author(s) received no specific funding for this work.

Data availability Some or all data, models or code that supports the findings of this study is available from the corresponding author upon reasonable request.

Declarations

Competing interests The authors declare that they have no competing interests.

References

Bagheri S, Kabiri-Samani A (2020a) Overflow characteristics of streamlined weirs based on model experimentation. Flow Meas Instrum 73:101720. https://doi.org/10.1016/j.flowmeasinst.2020.101720

Bagheri S, Kabiri-Samani A (2020b) Simulation of free surface flow over the streamlined weirs. Flow Meas Instrum 71:101680. https://doi.org/10.1016/j.flowmeasinst.2019.101680

Bai ZL, Peng Y, Zhang JM (2017) Three-dimensional turbulence simulation of flow in a V-shaped stepped spillway. J Hydraul Eng 143(9):06017011. https://doi.org/10.1061/(ASCE)HY.1943-7900.0001328

Bos MG (1976) Discharge measurement structures. Ilri

Chamani MR, Rajaratnam N (1999) Onset of skimming flow on stepped spillways. J Hydraul Eng 125(9):969–971. https://doi.org/10.1061/(ASCE)0733-9429(1999)125:9(969)

Ghaderi A, Abbasi S, Abraham J, Azamathulla HM (2020a) Efficiency of trapezoidal labyrinth shaped stepped spillways. Flow Meas Instrum 72:101711. https://doi.org/10.1016/j.flowmeasinst.2020.101711

Ghaderi A, Daneshfaraz R, Torabi M, Abraham J, Azamathulla HM (2020b) Experimental investigation on effective scouring parameters downstream from stepped spillways. Water Supply 20(5):1988–1998. https://doi.org/10.2166/ws.2020.113

Hager WH, Pfister M (2010) Hydraulic modelling—an introduction: principles, methods and applications. J Hydraul Res 48(4):557–558. https://doi.org/10.1080/00221686.2010.492104

Haghiabi A (2017) Estimation of scour downstream of a ski-jump bucket using the multivariate adaptive regression splines. Sci Iran Trans A Civ Eng 24(4):1789–1801

Haghiabi AH, Mohammadzadeh-Habili J, Parsaie A (2018) Development of an evaluation method for velocity distribution over cylindrical weirs using doublet concept. Flow Meas Instrum 61:79–83. https://doi.org/10.1016/j.flowmeasinst.2018.03.008

Haghiabi AH, Ghaleh Nou MR, Parsaie A (2022) The energy dissipation of flow over the labyrinth weirs. Alex Eng J 61(5):3729–3733. https://doi.org/10.1016/j.aej.2021.08.075

James CS, Matos J, Ohtsu I, Yasuda Y, Takahashi M, Tatewar Sandip P, Ingle Ramesh N, Porey Prakash D, Chamani MR, Rajaratnam N (2001) Onset of skimming flow on stepped spillways. J Hydraul Eng 127(6):519–525. https://doi.org/10.1061/(ASCE)0733-9429(2001)127:6(519)

Mohammad Rezapour Tabari M, Tavakoli S (2016) Effects of stepped spillway geometry on flow pattern and energy dissipation. Arab J Sci Eng 41(4):1215–1224. https://doi.org/10.1007/s13369-015-1874-8

Mohammadzadeh-Habili J, Heidarpour M, Haghiabi A (2016) Comparison the hydraulic characteristics of finite crest length weir with quarter-circular crested weir. Flow Meas Instrum 52:77–82. https://doi.org/10.1016/j.flowmeasinst.2016.09.009

Moukalled F, Mangani L, Darwish M (2015) The finite volume method in computational fluid dynamics: an advanced introduction with OpenFOAM® and Matlab. Springer, Cham

Nou MRG, Zolghadr M, Bajestan MS, Azamathulla HM (2021) Application of ANFIS–PSO hybrid algorithm for predicting the dimensions of the downstream scour hole of ski-jump spillways. Iran J Sci Technol Trans Civ Eng 45(3):1845–1859. https://doi.org/10.1007/s40996-020-00413-w

Parsaie A, Haghiabi AH (2019a) Evaluation of energy dissipation on stepped spillway using evolutionary computing. Appl Water Sci 9(6):144. https://doi.org/10.1007/s13201-019-1019-4

Parsaie A, Haghiabi AH (2019b) The hydraulic investigation of circular crested stepped spillway. Flow Meas Instrum 70:101624. https://doi.org/10.1016/j.flowmeasinst.2019.101624

Parsaie A, Haghiabi AH (2019c) Inception point of flow aeration on quarter-circular crested stepped spillway. Flow Meas Instrum 69:101618. https://doi.org/10.1016/j.flowmeasinst.2019.101618

Parsaie A, Haghiabi A (2021) Hydraulic investigation of finite crested stepped spillways. Water Supply 21(5):2437–2443. https://doi.org/10.2166/ws.2021.078

Parsaie A, Dehdar-Behbahani S, Haghiabi AH (2016) Numerical modeling of cavitation on spillway's flip bucket. Front Struct Civ Eng 10(4):438–444. https://doi.org/10.1007/s11709-016-0337-y

Parsaie A, Moradinejad A, Haghiabi AH (2018) Numerical modeling of flow pattern in spillway approach channel. Jordan J Civ Eng 12(1):1–9

Rahimzadeh H, Maghsoodi R, Sarkardeh H, Tavakkol S (2012) Simulating flow over circular spillways by using different turbulence models. Eng Appl Comput Fluid Mech 6(1):100–109. https://doi.org/10.1080/19942060.2012.11015406

Rajaratnam N (1990) Skimming flow in stepped spillways. J Hydraul Eng 116(4):587–591. https://doi.org/10.1061/(ASCE)0733-9429(1990)116:4(587)

Samadi M, Jabbari E, Azamathulla HM, Mojallal M (2015) Estimation of scour depth below free overfall spillways using multivariate adaptive regression splines and artificial neural networks. Eng Appl Comput Fluid Mech 9(1):291–300. https://doi.org/10.1080/19942060.2015.1011826

Shamsi Z, Parsaie A, Haghiabi AH (2022) Optimum hydraulic design of cylindrical weirs. ISH J Hydraul Eng 28(sup1):86–90. https://doi.org/10.1080/09715010.2019.1683474

Tadayon R, Ramamurthy AS (2009) Turbulence modeling of flows over circular spillways. J Irrig Drain Eng 135(4):493–498. https://doi.org/10.1061/(ASCE)IR.1943-4774.0000012

Valero D, Bung DB, Crookston BM (2018) Energy dissipation of a type III basin under design and adverse conditions for stepped and smooth spillways. J Hydraul Eng 144(7):04018036. https://doi.org/10.1061/(ASCE)HY.1943-7900.0001482

Wang J-b, Chen H-c (2010) Improved design of guide wall of bank spillway at Yutang Hydropower Station. Water Sci Eng 3(1):67–74. https://doi.org/10.3882/j.issn.1674-2370.2010.01.007

Zhan J, Zhang J, Gong Y (2016) Numerical investigation of air-entrainment in skimming flow over stepped spillways. Theor Appl Mech Lett 6(3):139–142. https://doi.org/10.1016/j.taml.2016.03.003

Zhang Q, Diao Y, Zhai X, Li S (2015) Experimental study on improvement effect of guide wall to water flow in bend of spillway chute. Water Sci Technol 73(3):669–678. https://doi.org/10.2166/wst.2015.523